QUANTIFYING THERMO-MECHANICAL STABILITY IN BINDER JETTING CORES: A STATISTICAL APPROACH WITH COATING AND ORIENTATION EFFECTS

Stefania Cacace, Paolo Parenti and Quirico Semeraro
Dipartimento di Meccanica, Politecnico di Milano, Via La Masa 1, 20156 Milan, Italy

Daniele Chiesa and Maurizio Chiesa
Fonder Shell S.r.l., Via Del Santuario 54 – Fraz. Strà Alta Val Tidone, 29031 Piacenza, Italy

https://doi.org/10.1007/s40962-026-01891-w

Abstract

Dimensional stability and thermo-mechanical performance are critical aspects of any core manufacturing process. Among additive manufacturing (AM) technologies, binder jetting is increasingly adopted in sand casting; understanding how process parameters affect these properties becomes particularly important. This study investigates the effect of printing configurations (i.e., part orientation and position inside the build box) and post-process steps (i.e., baking and coating) on the thermo-mechanical behaviour of furan binder-jetted silica mix sand cores using the Hot Distortion Test (HDT). Results show that core baking alone induces only modest modifications (≈ 20% increase in deflection and slope of the HDT curve, but negligible impact on printing anisotropy), whereas the application of a coating (with subsequent baking) substantially enhances thermal durability and extends the breakage time by ≈ 40% on average without increasing maximum deflection. More importantly, coating mitigates the strong anisotropic behaviour of vertically printed specimens, reducing the performance gap with planar orientations, with deflection differences dropping from ∼ 25 to ∼ 12% after coating. Multivariate regression analysis consistently highlights the printing orientation of the parts and post-process as the main significant factors across both experiments, while the part location inside the printer build box has only a minor or inconsistent effect. To improve the analysis, an HDT-area descriptor is designed and adopted, which aggregates multiple curve features into a single metric. Regression models based on HDT-area confirm the same significant factors while providing excellent explanatory power (Adj-R^2 up to 85%) and reducing printing orientation-dependent variability. These findings indicate that coating not only prolongs core durability but also reduces part-to-part variability, while HDT-area emerges as a reliable synthetic indicator for design and quality assurance in AM-enabled foundry workflows.

Keywords: *binder jetting, sand cores, hot distortion test, coating, furan binder, thermo-mechanical behaviour*

Introduction

Among the many additive manufacturing technologies available, binder jetting has become increasingly integrated into sand casting processes; understanding the thermo-mechanical performance of 3D-printed cores is essential for ensuring dimensional stability and casting quality of highly complex geometries. Binder jetting (BJ) is an AM method that is increasingly adopted for core production. BJ method enables complex geometries, eliminating the need for traditional patterns or core boxes and ensuring high-dimensional accuracy and surface quality through optimized sand characteristics and process parameters. This process, however, introduces unique features in terms of anisotropy and spatial variability, due to the layer-by-layer deposition process.[1] Consequently, the final properties of printed cores—such as thermal resistance and thermal expansion behaviour—can vary depending on part orientation and location within the build area.

Coating is commonly applied to sand cores to reduce surface defects in castings, but its role extends beyond simply improving surface finish. When applied to cores, coating

Received: 24 October 2025 / Accepted: 23 January 2026
Published online: 25 February 2026

may influence not only interfacial phenomena during casting, but also the mechanical and thermal behaviour of the core itself, potentially affecting the final core functional properties.[2,3] Research demonstrates that coated cores show much smaller sensitivity to thermal deformation and maintain resistance to high temperatures. The coating provides additional thermal protection, creating a thermal integrity barrier between the molten metal and sand core[4] Coating prevents metal penetration into the sand structure, a critical improvement given the lower compaction density of 3D-printed cores compared to standard shot cores. The packing density in 3D-printed cores varies with printing direction and is generally lower than conventional cores, making them more susceptible to metal penetration without coating protection.[5] The refractory coating fills voids and creates an impervious barrier between the molten metal and sand surface. This barrier function is essential for preventing sand burn-in, metal–mould reactions, and other surface defects that would otherwise compromise casting quality.[6] The optimal coating formulations depend on many aspects that include functional performance, costs, but also environmental conditions. Among the types of coatings, water-based coatings represent the environmentally preferred option, eliminating VOC emissions and hazardous material-handling concerns. Due to the specific characteristics of 3D-printed cores, some coating material suppliers propose specific formulations for BJ cores that are declared to boost the final 3D cores' properties.[7,8] Unfortunately, no available scientific information can be found that can support the declared superior performances on the 3D-printed cores.

Although some previous studies discuss the beneficial effects of coating 3D-printed cores, there are still open concerns regarding the interaction between coating effectiveness and AM-induced variability, which remains poorly understood—despite its relevance in the industrial context of high-volume production of 3D-printed cores.

To assess the influence of the coating on the mechanical properties of 3D-printed sand cores, this study utilized the Hot Distortion Test (HDT). HDT test provides a direct measure of the thermo-mechanical stability of printed cores under load, making it particularly suitable for assessing deformation behaviour near casting temperatures.[9] The effect of coatings on the thermo-mechanical behaviour of traditionally manufactured sand cores using the HDT was investigated by Jakubski et al.[10] and Budávari and Varga.[11] The test curves were evaluated using two primary indicators: maximum deformation and time to degradation. Jakubski et al.[10] found that the type of coating significantly affected thermal deformation, whereas coating thickness had little impact. Budavári and Varga[11] demonstrated that higher curing temperatures and longer curing times increased core brittleness and thermal distortion, highlighting the need to balance curing parameters to maintain dimensional stability. Other relevant studies, including those by Nwaogu et al.[12], Jamrożowicz and Siatko,[13] Liu et al.[14], and Kaźnica and Zych,[15] focused on various aspects of coating performance, such as surface quality improvement, permeability, gas evolution, and moisture resistance. Nwaogu et al.[12] showed that the application of sol–gel coatings on cores enhances surface integrity by providing uniform coverage and moderate penetration. The coating contributes to thermal crack resistance and strengthens the core surface, improving its protective barrier against molten metal. According to Liu et al.[14], optimized water-based coatings result in dense films with fast drying, low gas evolution, and high surface strength. These properties enhance the thermal and mechanical stability of the core, reducing the risk of gas-related defects during casting. Kaźnica and Zych[15] found that coating viscosity, sand grain size, and application method significantly affect the coating thickness and penetration into the core. Higher-viscosity coatings produce thicker surface layers with lower penetration, which influences the mechanical protection and reactivity of the core during metal contact. A summary of the presented literature can be found in Table 1.

Importantly, all studies relied on conventionally manufactured cores rather than BJ, and therefore open questions remain uncleared regarding the coating effect on 3D-printed cores. As such, their findings, while informative, do not directly address the material anisotropy induced by locations and printing orientation characteristic of 3D-printed cores, which are central to the present study.

This work aims to evaluate how post-process steps of 3D-printed cores (such as baking and coating) interact, in terms of thermo-mechanical behaviour (HDT testing), with printing strategies. Rather than focusing on the coating performance in absolute terms, this study points to its relative effect across a set of samples printed at different build height and with different printing orientation. Understanding these interactions supports the development of robust process guidelines and informed decisions about post-process treatments in AM-based sand cores. The followed approach leverages a robust statistical evaluation of the HDT curves, whereas different synthetic indicators are extracted from them to allow a precise quantification of the effects of each factor. This method and the outlined results are believed to be particularly relevant for core-making and casting industries, where consistency and predictability across the 3D printer build volumes are unquestionably critical. With respect to the state of the art, this work uses a statistically sound methodology to evaluate the influence of printing strategies on the thermo-mechanical properties of sand cores. In addition, we present a complete analysis of the HDT curves through the analysis of multiple characteristic points that capture key aspects of core behaviour. Finally, we propose a new indicator, the area under the HDT curve, which consolidates these characteristic points into a single quantitative measure, providing an effective

Table 1. Summary of Literature Investigating the Effect of Coatings on the Thermo-Mechanical Behaviour of Conventionally Manufactured Sand Cores

	Type of coating	Measured characteristics	Main results
Nwaogu et al.[12]	Sol–gel refractory	Surface quality, coating adhesion, veining index, penetration depth	New sol–gel coatings improved casting surface quality and reduced surface defects significantly.
Jamrozowicz and Siatko[13]	Zircon alcohol-based coatings	Permeability under different conditions, coating thickness	Coating reduced permeability; effectiveness depended on base sand and application parameters.
Liu et al.[14]	Water-based coatings with optimized refractory aggregates and binders	Drying time, gas volume, wear loss, SEM analysis	Coatings showed high strength, low gas evolution, and fast drying.
Kaźnica and Zych[15]	Zirconium and zirconium–graphite (alcohol-based)	Moisture uptake (gravimetric and ultrasonic methods)	Coatings reduce moisture uptake, especially with one layer; performance varies with sand type.
Budavári and Varga[11]	Resin coating	Hot distortion (deformation, degradation time)	Higher curing temperatures/time increases deformation.
Jakubski et al.[10]	Graphite, aluminium–silicate	Hot Distortion Test (thermal deformation during baking)	Coating type significantly affects thermal behaviour.

way to assess the impact of printing strategies on the HDT response.

Materials and Methods

Binder Jetting for Sand Printing

HDT specimens were printed using an ExOne S-Max Pro BJ system. The main process parameters are reported in Table 2. The BJ process produces sand moulds and cores directly from CAD models by selectively depositing a liquid binder onto thin layers of sand. The process involves the selective deposition of micro-droplets of a furan-based binder onto a thin layer of permeable silica sand pre-mixed with an activator. A printhead jets the binder in precise locations according to the geometry of each cross section. After each layer, the platform lowers, and a new layer of sand is spread, repeating the cycle until the object is fully formed.

The activator in the sand acts as a catalyst: When the sprayed binder comes into contact with it, the cross-linking reaction is initiated, allowing the material to harden sufficiently to enable de-sanding and removal from the build box. The adopted binder is a furan-based resin, a no-bake technology commonly used in sand 3D printing for foundry applications. The catalyst supplied by ExOne is based on paratoluenesulphonic acid. After printing, the cores are de-sanded and stored to allow the hardening process to stabilize before HDT testing. The sand system consisted of a mixed silica–ceramic blend composed of ExOne silica sand FS001 and Cerabeads FS055 form sand. The combination of silica and ceramic sands was selected to balance thermal stability and dimensional accuracy, taking advantage of the low cost and availability of silica sand together with the reduced thermal expansion and improved refractoriness of ceramic beads. The sand granulometry ranges from 20 to 170 μm, corresponding to the 10th and 90th percentiles of the circular equivalent diameter distribution, measured using a Malvern Morphologi G4.

Table 2. BJ Printing Properties and Settings

Machine settings	Values
Build box dimension	1800 mm x 1000 mm x 700 mm
Z-resolution (layer height)	0.28 mm
X-resolution	0.14
Recoater speed	155 mm/s
Chamber temperature	32°C
Binder type	Furan-based
Catalyst %	0.19%
Sand type	Silica–ceramic blend

HDT Test and Curve Characterization

Hot Distortion Tests were conducted using a commercial device, the Benetlab Hot FLEX. This setup includes a gas burner as the heat source, a specimen holder, and a contact linear displacement sensor (linear variable differential transformer, LVDT) with a spatial resolution of 0.01 mm. HDT were performed by applying a load of 40 g at the specimen edge. The thermal load was controlled by fixing the air/gas mixing parameters of the heating system. The HDT specimens used in the experiments have a prismatic shape, measuring 170 × 42 × 8.5 mm, as illustrated in Figure 1.

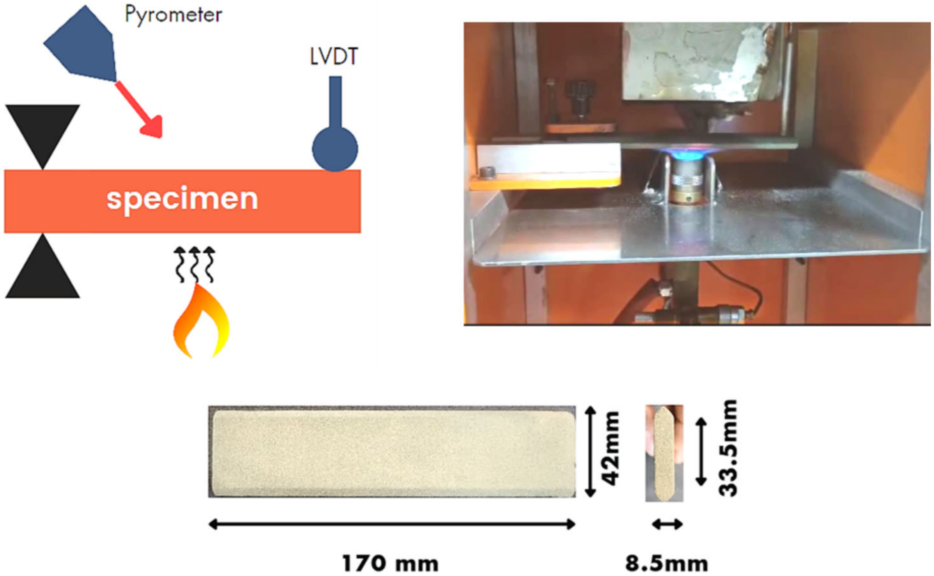

Figure 1. HDT testing procedure: experimental equipment and tested geometries.

The typical HDT curve for BJ specimens is shown in Figure 2. The curve usually presents a steep increase in deflection at the beginning of the test; as the heat builds up, the deflection reaches a steady condition which corresponds to the maximum deflection. Then, right before rupture, the specimen starts collapsing, and the deflection shows a downward trend. To characterize fully the HDT curve, it is possible to analyse some critical features, which are listed in Table 3. For a detailed review of the analysis of the indicators in the HDT curves, the reader is referred to the authors' previous work.[16]

It must be noted that to properly analyse the curve features, multivariate statistical tools are needed to account for the correlation between them.[17] To capture the combined influence of the initial steep increase in deflection, the length of the plateau, the breakage time, and the maximum deflection in a single metric, a specific indicator is identified and analysed, which consists of the HDT area (simply called here on area)**.** This indicator consists of the area under the HDT curve from the beginning of the test until collapse (e.g., the blue area in Figure 2).

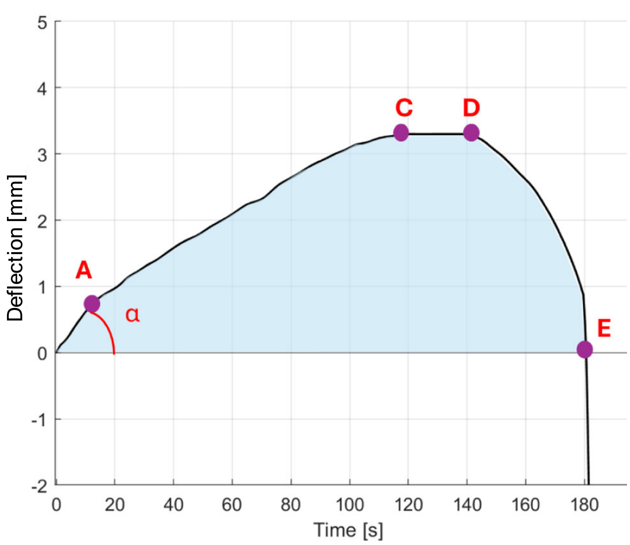

Figure 2. Example of HDT curve, curve features from Table 3, and HDT-area indicated as a blue region.

Because the area indicator weights both duration and magnitude, it is sensitive to improvements (or degradations) that a single-point feature can miss (e.g., an increase in the breakage time while maximum deflection is constant). This newly adopted metric has two practical advantages:

- **Noise immunity.** Numerical integration smooths local oscillations, which can be due to the adopted contact sensor.
- **Statistical parsimony.** Later regressions use one response instead of four, reducing Type-I error (i.e., false positive—in our case declaring a factor significant when it is not) without sacrificing the explanatory power.

Post-Processing

The specimens were taken for coating and baking 24 hours after printing.

Coating

The coating mixture consisted of a water-based ceramic slurry based on aluminium silicates, with fixed composition and temperature. The slurry was contained in a mixing tank and continuously kept under agitation by rotating blades to ensure uniformity and to prevent sedimentation. Its density was continuously monitored and maintained between 26 and 32 Baumé by adjusting the water and powder content. The coating was applied by a manual immersion (dip-coating) process under constant laboratory temperature and humidity conditions. The specimens were placed in a metallic tray and dipped into the slurry. The immersion time was set approximately at 4 s, and a single dipping cycle was employed for all samples.

Figure 3 shows a SEM micrograph of a fractured cross section of a coated specimen. Sand particles with a typical grain size in the range of 100–200 µm can be clearly observed. A distinct coating layer is visible, characterized by much finer and more irregular particles compared to the underlying sand. The coating penetrates approximately 180 µm from the internal surface into the core. By effectively covering and masking the sand grains, the coating smooths the surface profile, resulting in a more uniform core surface and potentially contributing to an improvement in the final casting surface roughness.

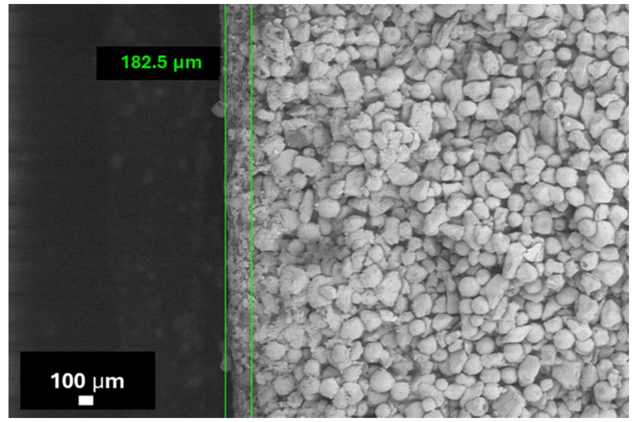

Figure 3. SEM micrograph of a fractured cross section of a coated sand core.

Baking

After dipping, the specimens were baked to dry and harden the applied coating as follows: they were stacked using multiple setters and placed in an electric furnace preheated to 120 °C. They were held at this temperature for 2 h, then removed from the furnace, and allowed to cool naturally to ambient temperature. Finally, the specimens were stored in a humidity-controlled room and tested within 48 h of the coating process.

During the experiments, the same baking procedure was also applied to the uncoated cores, even though the adopted technology was a no-bake furan system. This was done to verify whether an additional drying/hardening step could induce beneficial changes in the thermo-mechanical properties of the cores, thereby isolating the effect of the thermal treatment from that of the coating itself.

Experimental Plan

To investigate the effect of baking and coating on the thermal response of the specimens, two independent, yet structurally identical, experimental campaigns were designed. In both experiments, the same factors were varied: part orientation during printing (“orientation”) at three levels (X, Y, Z) and vertical location inside the building platform (“height”) at three levels (bottom, middle, top, whereas bottom indicates the position closer to the platform).

In each campaign, a set of HDT specimens was tested in “as-built” condition in order to assess the influence of the post-processing compared to the “base-case”, i.e., no post-processing. For each unique combination of orientation and height, at least two replicates were produced.

The three printing orientations are defined as follows:

<u>Orientation</u>

- X-axis: longitudinal direction perpendicular to the sand deposition
- Y-axis: direction of the sand deposition
- Z-axis: vertical printing direction

The three vertical locations are defined as follows:

<u>Height</u>

- Top: 370 mm from the build box base
- Middle: 175 mm from the build box base
- Bottom: 5 mm from the build box base

Three different groups of specimens were produced as indicated in Figure 4.

1) “Not baked” (NB) / “not coated” (NC): specimens that were HDT-tested without any post-processing.
2) “Baked” (B): specimens which were subjected to coating and baking, as described in Sects. 2.3.1 and 2.3.2.
3) “Coated” (C): specimens which were baked and coated, as described in Sect. 2.3.1.

Data Analysis

Statistical analysis aims to determine which factors influence the HDT response of the specimens, with a particular interest in understanding whether and to which extent the post-processes (baking and coating) influence the HDT curves and therefore the thermo-mechanical response of sand cores.

A multivariate regression analysis is carried out to determine the significant factors affecting HDT features defined in Table 3.

In the following tables and figures, the significance of each factor is reported using the following notation: *** indicates $p < 10^{-4}$, ** indicates $p < 0.001$, * indicates $p < 0.05$, and 'n.s.' denotes non-significant effects. The sign associated with each factor represents the direction of the effect with respect to the defined base case.

Results and Discussion

Baking Experiment

Figure 5 illustrates the HDT curves for the baked and not baked cases; for this experiment, 17 specimens were subject to baking and 17 specimens were analysed in the not-baked condition, for a total of 34 specimens. The ANOVA tables for the regressions are reported in Appendix A, while Table 4 summarizes the results of the statistical analysis.

For the baked case, there is a clear outlier curve in the Y direction. This condition shows a steeper initial increase in deflection (α) and a larger maximum deflection compared to its replicates. This sample was removed from the statistical analysis.

The analysis reveals that baking has a limited impact on the main features of the HDT curves, especially when compared to printing orientation, which consistently emerges as the dominant factor. As illustrated in Figure 5 and confirmed by regression results (Table 4), specimens printed along the Z direction show markedly different behaviour, with higher maximum deflection and α values, and earlier breakage times, regardless of the post-process treatment. In contrast, specimens printed in X and Y directions behave similarly. Similar results were obtained by the authors in.[16]

From a practical perspective, this confirms that anisotropic behaviour due to printing orientation is not mitigated by baking the cores. Therefore, in the design phase, the printing orientation of the part on the build platform remains the key driver of mechanical and thermal performance. The baking

Table 3. HDT Curve Features Analysed, Taken from the Previous Author's Work[16]

Curve feature	Point on the curve	Meaning
α	Slope from initial point (0,0) to A. A indicates the end of the initial increase in deflection.	The slope of the linear increase ending at point A.
ΔCD	C identifies the beginning of the steady region, while D is the point before the specimen starts collapsing	The time duration of the stable region, namely, the time interval between points C and D.
Max deflection	Usually is the deflection value in correspondence of C and D	The maximum positive deflection reached, typically coinciding with the ΔCD plateau.
Breakage time	The time coordinates of point E, which is the point where the displacement is back to 0.	The time at which the specimen collapses

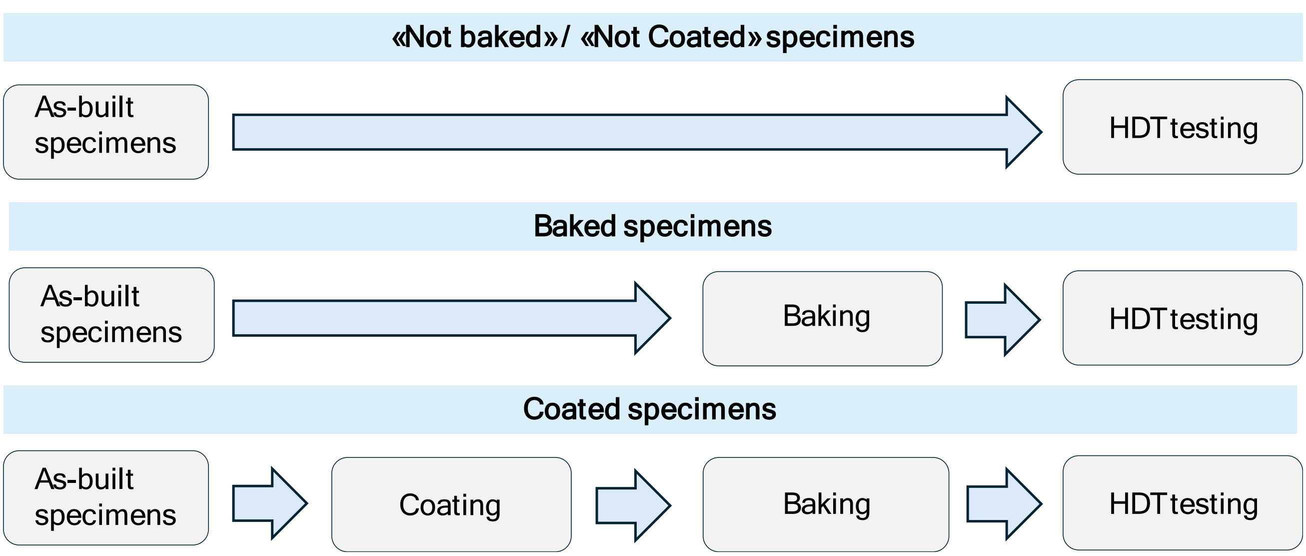

Figure 4. Post-processing workflow for the three types of conditions tested: "not-baked"/ "not-coated" specimens, baked specimens, and coated specimens.

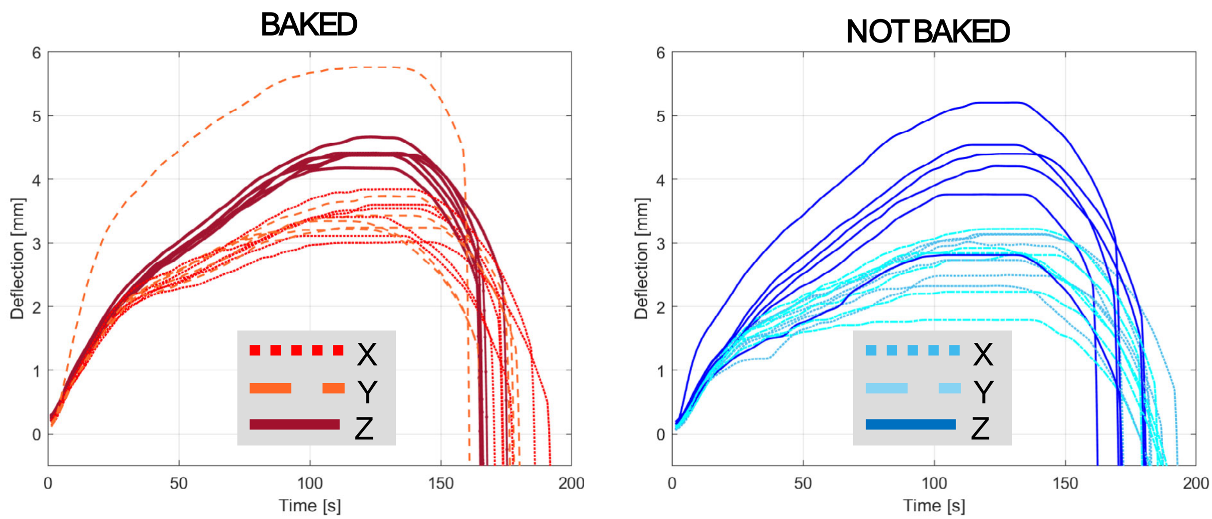

Figure 5. HDT results for the baking experiment.

process does induce statistically significant increases in max deflection and α and a slight reduction in breakage time, as shown in Table 5. The effect of the baking in terms of breakage time is between 3 and 5 seconds, which is about 2% of the average curve length. Instead, the deformation is increased by 20% in X and Y directions and by 10% in the Z direction. Similarly, the slope of the curve is increased by 20% in all directions due to baking alone. However, these effects are less influential than those due to orientation. X- and Y-oriented cores behave similarly; instead, the Z-oriented cores show a lower breakage time, with a difference of 11 s with the X orientation and 5.4 s with the Y orientation. The maximum deflection is significantly higher for the Z orientation, with an increased deflection of 1 mm compared to X and Y orientations.

Table 4. The Significant Factors for the Baking Experiment

	Breakage time (s)	α (mm/s)	Max deflection (mm)	ΔCD (s)
Direction Y	n.s.	n.s.	n.s.	n.s.
Direction Z	** (−)	** (+)	*** (+)	n.s.
Post-process	* (+)	*** (−)	*** (−)	n.s.
Height	n.s.	n.s.	n.s.	n.s.

The sign indicates the positive or negative effect of the factor on the response in respect of the "base case". For factor orientation, the base case is direction X, while for post-process the base case is "no treatment"

Notably, the variability of the curves, especially along the Z direction, is visibly reduced with baking (Figure 5), suggesting a potential homogenization effect. This could be relevant when consistency is prioritized over peak performance. The height factor, representing the distance from the build platform, was not statistically significant in this experiment.

In summary:

- Part orientation significantly affects HDT curve features, particularly for Z-oriented specimens.
- Baking modifies some curve characteristics but does not eliminate anisotropy.
- Part orientation should remain the primary consideration during process planning for thermo-mechanical performance optimization.

Table 5. Summary Statistics of Curve Features for the Baking Experiments

Orientation	Post-process	Breakage time (s)	α (mm/s)	Max deflection (mm)	ΔCD (s)
X	Baked	178.6 ± 8.2	0,0868 ± 0.004	3.5 ± 0.4	29.3 ± 9.7
	Not-baked	182.0 ± 7.2	0,0644 ± 0.004	2.8 ± 0.3	31.9 ± 6.3
Y	Baked	172.9 ± 7.0	0,0870 ± 0.004	3.4 ± 0.2	27.5 ± 5.8
	Not-baked	182.0 ± 3.2	0,0660 ± 0.005	2.6 ± 0.5	30.2 ± 10.6
Z	Baked	167.5 ± 3.9	0,0918 ± 0.005	4.4 ± 0.2	22.5 ± 4.9
	Not-baked	172.7 ± 7.6	0,0719 ± 0.007	3.9 ± 0.7	26.4 ± 8.4

Data are reported as Mean ± 1 Standard deviation

Coating Experiment

Figure 6 represents the HDT curves obtained in the coated and not coated case; for this experiment, 28 specimens were subject to coating, and an equal number is analysed in the not-coated condition, for a total of 56 specimens. The ANOVA tables for the regressions are reported in Appendix B, while Table 6 summarizes the results of the statistical analysis.

The results clearly show that coating has a strong impact on the mechanical and thermal behaviour of the specimens, particularly in terms of breakage time and ΔCD. Coated specimens consistently resist thermal stress for significantly longer durations, without increasing their max deflection.

In particular, the breakage time is increased by almost 40% in all directions due to coating, while the difference in max deflection is around 5% (see Table 7). This is a key finding from a design standpoint: the structural integrity is preserved while extending functional life, which translates into enhanced thermal endurance without compromising dimensional stability. This suggests that post-processing creates a protective layer that delays failure but does not modify the maximum deformation reached by the core. Practically, this allows for more robust cores in thermal environments without altering geometric tolerances. Additionally, coating appears to mitigate the anisotropic effects introduced by the printing process. The difference in behaviour between the Z direction and the other orientations is less pronounced in coated specimens, indicating that post-processing can reduce orientation-dependent variability. Without coating, on average, Z-oriented cores resulted in a 3.8 mm max deflection, 25% higher than X/Y-oriented cores; after coating, on average, Z-oriented cores show a max deflection of 3.5 mm, only 12% higher than X/Y orientation. This opens new opportunities for design freedom, allowing more flexible positioning of parts on the build platform without severely impacting the thermo-mechanical performance. While height shows some minor significance (notably for max deflection), its effect is less consistent and secondary. The impact of Y direction remains ambiguous, with significance limited to certain features (α and max deflection) and relatively low effect sizes.

Table 6. The Significant Factors for the Coating Experiment

	Breakage time (s)	α (mm/s)	Max deflection (mm)	ΔCD (s)
Y direction	n.s.	* (−)	* (−)	n.s.
Z direction	*** (−)	n.s.	*** (+)	n.s.
Post-process	*** (+)	*** (+)	n.s.	*** (+)
Height	n.s.	n.s.	** (−)	n.s.

The sign indicates the positive or negative effect of the factor on the response with respect to the "base case". For factor orientation, the base case is direction X, while for post-process the base case is "no treatment"

Importantly, the observed improvements cannot be attributed to the baking step alone, as similar effects were not observed in the baking-only experiment. This confirms that the observed changes are indeed due to the coating treatment.

In summary:

- Coating significantly increases thermal durability (breakage time, ΔCD) without affecting maximum deformation.
- Anisotropies due to build orientation are reduced, especially for Z-printed parts.
- Designers can exploit coating to enhance thermal performance and reduce process-induced variability.

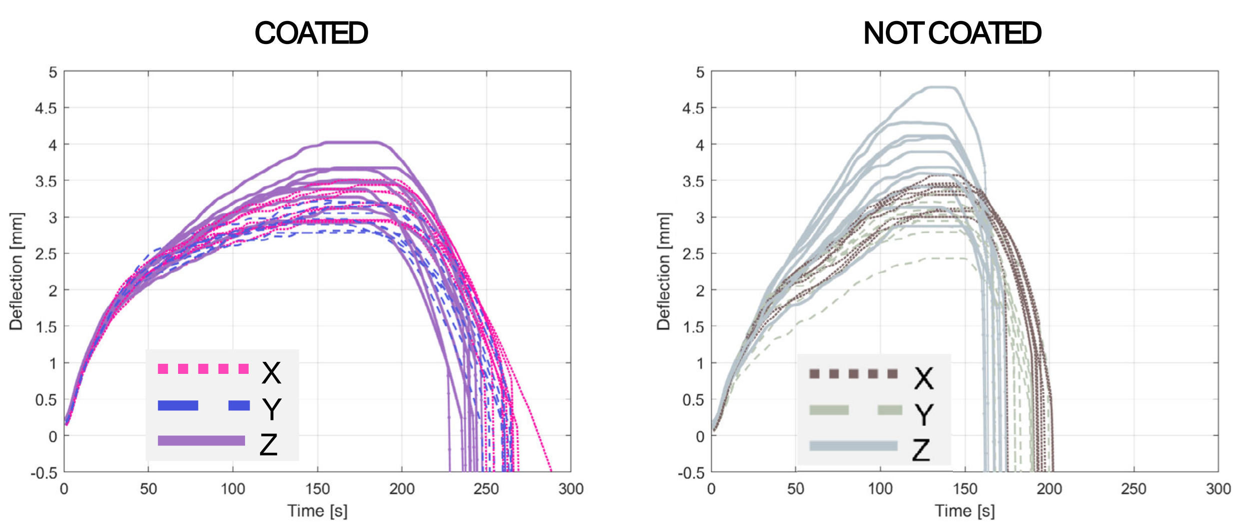

Figure 6. HDT results for the coating experiment.

Table 7. Summary Statistics of Curve Features for the Coating Experiment

Orientation	Post-process	Breakage time (s)	α (mm/s)	Max deflection (mm)	ΔCD (s)
X	Coated	261.8 ± 8.3	0.0786 ± 0.004	3.2 ± 0.2	41.6 ± 16.9
	Not coated	193.0 ± 7.9	0.0674 ± 0.004	3.3 ± 0.2	26.3 ± 6.7
Y	Coated	257.9 ± 5.9	0.0751 ± 0.003	3.0 ± 0.2	43.2 ± 6.2
	Not coated	185.3 ± 9.0	0.0635 ± 0.006	3.0 ± 0.3	29.7 ± 8.8
Z	Coated	232.2 ± 24.4	0.0789 ± 0.008	3.5 ± 0.3	37.3 ± 11.9
	Not coated	167.3 ± 4.2	0.0716 ± 0.005	3.8 ± 0.6	26.9 ± 8.9

Data are reported as Mean ± 1 Standard deviation

Table 8. Regression Table for the HDT-Area in the Baking Experiment (Adj-R^2 = 62.00%)

Area (mm*s)	Coeff	p value	
Regression		1.3e−06	***
Intercept	457.42	<2e−16	***
Y direction	− 14.60	0.494	
Z direction	94.56	1e−04	**
Post-process	− 80.02	7.7e−05	***
Height	− 17.91	0.100	

***Indicates a p value $<10^{-4}$, **p value < 0.001, and *a p value <0.05

Table 9. Regression Table for the HDT-Area in the Coating Experiment (Adj-R^2 = 85.52%)

Area (mm*s)	Coeff	p value	
Regression		<2e−16	***
Intercept	455.12	<2e−16	***
Y direction	−53.95	1.7e−04	**
Z direction	−10.41	0.438	
Post-process	183.40	<2e−16	***
Height	−27.43	0.001	**

***Indicates a p value $<10^{-4}$, **p value < 0.001, and *a p value <0.05

- Analysing HDT curves based on a single feature may lead to misleading conclusions; a multivariate view is essential.

New Approach: Area-Based Metric for HDT Test

The selection of the curve features (Table 3) might be time-consuming and sometimes also not straightforward, for example, the selection of points A and C might not be clear due to the small variation of the curve (Figure 2). For quality assurance policies, it would be easier to use a more automatic and simple approach. For this reason, we introduce the area under the curve as a unique factor of interest to characterize the thermal response of the material during the HDT test.

Given that only one feature is analysed, a simple linear regression can be used to estimate the effects of orientation, height, and post-process on the area of the curve. The calculation of the area under the curve can also be performed easily also in Excel or with a simple and automatic code (such as Python or MATLAB) that can be integrated in the HDT apparatus. This procedure was implemented for both baking and coating experiments. The resulting models from the analysis of area for the baking and coating experiments are reported in Tables 8 and 9.

First, the quality of the models using area as the response is quite high, particularly in the coating experiment. The significant factors identified when considering area are the same as those found when analysing the four curve features (see Tables 4 and 6). This indicates that reducing the number of response variables (from four to just one) does not lead to a loss of information from the experiment.

In Figure 7, the main effect plots of the area for the baking and the coating experiments are shown; the y-axis is the same for both graphs to allow a direct comparison between the two experiments. The main effects plot displays the means of the area for the different levels of orientation, post-process, and height. The average area is clearly higher in the coating condition, which results in longer curves and thus larger areas. Furthermore, the area indicator shows that the effect of orientation is reduced in the coating experiment, consistent with the findings from the individual HDT curve features. The homogenization effect of the coating post-process is also evident in the area, as the differences in area across the different orientations are clearly reduced. This is a key result that reinforces the idea of using area instead of multiple individual features. Also, certain features, such as ΔCD in the baking experiment (Adj-R^2 ≈ 5%), showed very low explanatory power, suggesting that their use as standalone descriptors may be of limited practical value, making the use of the area a

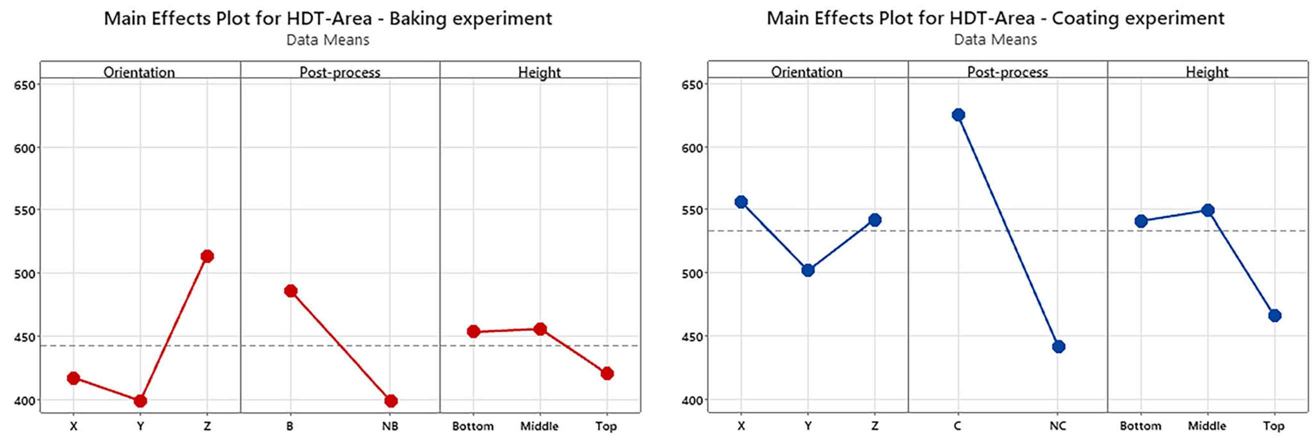

Figure 7. Main effect plot of HDT-area for the baking experiment (left) and for the coating experiment (right). Each dot represents the mean value of the HDT-area for the curves for the corresponding value on the x-axis. The labels on the x-axis refer to: B (baked), NB (not baked), H (heated), NH (not heated). Both plots use the same y-axis to ease comparison.

more valuable indicator. Moreover, it is noteworthy that in the coating experiment, relying solely on breakage time or max deflection would not have provided a complete understanding of the post-processing effects. By using area, differences in the overall 'shape' of the curve can be detected, enabling a more comprehensive analysis of how all variables influence the HDT curve. Additionally, this approach simplifies the preprocessing step by eliminating the need to select specific points on the curve.

Since it is not always possible to predict which curve feature will be affected by a given post-treatment or process variation, using area offers a faster and more reliable method for detecting potential effects on the thermo-mechanical properties.

Conclusion

This study quantified the influence of two common post-processes, baking and refractory coating, on the hot distortion performance of binder-jetted silica sand cores. Printing orientation consistently emerged as the dominant factor, with Z-oriented specimens showing higher deflections and shorter lifetimes compared to X/Y-oriented ones. Baking alone produced only modest changes—slightly increasing deflection and slope—without alleviating anisotropy. In contrast, coating markedly improved thermal durability, extending breakage time by approximately 40% while keeping maximum deflection unchanged. Importantly, coating also reduced orientation-dependent variability—from about 25 to 12%—thereby enhancing design freedom in part placement.

From a methodological perspective, multivariate regression confirmed orientation and post-process as the only robustly significant factors across all curve features, while height played only a minor role. Furthermore, the introduction of the area descriptor provided a powerful synthetic indicator: it retained the same significant factors as the classical curve features but with higher explanatory power and simpler implementation. The area thus represents a practical quality-monitoring tool, offering both robustness against noise and reduced risk of spurious statistical findings.

Overall, the results highlight coating as an effective strategy to improve both durability and process robustness of AM sand cores, while the proposed area approach enables a more reliable and streamlined assessment of thermo-mechanical stability in industrial practice.

Funding

Open access funding provided by Politecnico di Milano within the CRUI-CARE Agreement.

Conflict of interest The authors have no relevant financial or nonfinancial interests to disclose.

Appendix A: ANOVA Tables for Baking Experiments

See Tables 10, 11, 12 and 13.

Table 10. Regression Table for Breakage Time in the Baking Experiment (Adj-R^2 = 37.34%)

Breakage time	Coeff	*p* value	
Regression		0.001	**
Intercept	177.330	<2e−16	***
Direction Y	−2.683	0.325	
Direction Z	−10.119	0.001	**
Post-process	5.917	0.012	*
Height	−0.488	0.718	

Table 11. Regression Table for α in the Baking Experiment (Adj-R^2 =82.73 %)

α	Coeff	*p* value	
Regression		1.77e−11	***
Intercept	0.0861	<22−16	***
Direction Y	0.001	0.666	
Direction Z	0.006	0.006	**
Post-process	−0.021	7.6e−13	***
Height	−0.001	0.562	

Table 12. Regression Table for Maximum Deflection in the Baking Experiment (Adj-R^2 = 69.35%)

Max deflection	Coeff	*p* value	
Regression		6.4e−08	***
Intercept	3.471	<2e−16	***
Direction Y	−0.147	0.398	
Direction Z	1.014	1e−16	***
Post-process	−0.612	9.1e−05	***
Height	−0.095	0.261	

Table 13. Regression Table for ΔCD in the Baking Experiment (Adj-R^2 = 5.15%)

ΔCD	Coeff	*p* value	
Regression		0.244	
Intercept	29.097	5.5e−12	***
Direction Y	−1.768	0.590	
Direction Z	−6.273	0.064	
Post-process	3.000	0.272	
Height	1.105	0.502	

Appendix B: ANOVA Tables for Coating experiments

See Tables 14, 15, 16, and 17.

Table 14. Regression Table for Breakage Time in the Coating Experiment (Adj-R^2 = 89.98%)

Breakage time	Coeff	*p* value	
Regression		<2e−16	***
Intercept	191.828	<2e−16	***
Direction Y	−5.813	0.157	
Direction Z	−27.293	1.2e−08	***
Post-process	68.748	<2e−16	***
Height	−3.541	0.135	

Table 15. Regression Table for α in the Coating Experiment (adj-R^2 = 50.48%)

A	Coeff	*p* value	
Regression		5e−08	***
Intercept	0.068	<2e−16	***
Direction Y	−0.004	0.041	*
Direction Z	0.002	0.227	
Post-process	0.010	1.1e−08	***
Height	−0.001	0.062	

Table 16. Regression Table for Max Deflection in the Coating Experiment (adj-R^2 = 48.40 %)

Maximum deflection			
	Coeff	*p* value	
Regression		1.4e−07	***
Intercept	3.259	<2e−16	***
Direction Y	−0.274	0.011	*
Direction Z	0.411	2e−04	***
Post-process	−0.149	0.083	
Height	−0.189	0.003	**

Table 17. Regression Table for ΔCD in the Coating Experiment (adj-R2 = 59.74%)

ΔCD			
	Coeff	*p* value	
Regression		2e−04	***
Intercept	28.585	1.5e−13	***
Direction Y	2.513	0.464	
Direction Z	−2.348	0.489	
Post-process	13.010	2e−05	***
Height	3.384	0.090	

REFERENCES

1. F. Wang, X. Cui, Q. Yang, H. Song, D. Li, Fabrication and posttreatment for inorganic binder jetting sand molds for casting. Addit. Manuf. **73**, 103690 (2023). https://doi.org/10.1016/j.addma.2023.103690
2. G.I. Cubillos, M.E. Mendoza, J.E. Alfonso, G. Blanco, M. Bethencourt, Chemical composition and microstructure of zirconium oxynitride thin layers from the surface to the substrate-coating interface. Mater Charact **131**, 450–458 (2017). https://doi.org/10.1016/j.matchar.2017.07.035
3. S. Yao, T. Wang, Improved surface of additive manufactured products by coating. J. Manuf. Process. **24**, 212–216 (2016). https://doi.org/10.1016/j.jmapro.2016.09.007
4. U.C. Nwaogu, N.S. Tiedje, Foundry coating technology: a review. Mater. Sci. Appl. **02**(08), 1143–1160 (2011). https://doi.org/10.4236/msa.2011.28155
5. N. Tshabalala, K. Nyembwe, M. Van Tonder, Optimisation of a resin-coated chromite sand for rapid sand casting applications. South Afr. J. Ind. Eng. **32**(3), 290–298 (2021). https://doi.org/10.7166/32-3-2665
6. B. Omidiji, A. Ajewole, and A. Oluwajobi, *Refractory coating technology: a review* (2024). 10.5281/ZENODO.13682958
7. Foseco India Ltd., "Reduction of rework and scrap with the new TENO PRINT coating for the 3D printing process." Accessed: Oct. 20, 2025. https://gifa.foseco.com/hubfs/TENO%20PRINT%20case%20study.pdf
8. Hüttenes-Albertus, "Coatings for additively manufactured moulds and cores (2019). Accessed: Oct. 20, 2025. https://www.ha-group.com/en/media/news-technical-articles/detail/coatings-for-additively-manufactured-moulds-and-cores/
9. M. Stachowicz, Modified hot distortion test to investigate the effect of the inorganic binder on the high-temperature behaviour of physically hardened moulding sands. Arch. Foundry Eng. (2018). https://doi.org/10.24425/122501
10. J. Jakubski, S.M. Dobosz, P. Jelinek, The influence of the protective coating type on thermal deformation of casting cores. Arch. Fundry **5**(15), 164–169 (2024)
11. I. Budavári, L. Varga, The effect of coremaking parameters on the thermal distortion behaviour of resin-coated sand. Hugarian Mater. Chem. Sci. Eng. **45**(1), 37–49 (2020)
12. U.C. Nwaogu, T. Poulsen, R.K. Stage, C. Bischoff, N.S. Tiedje, New sol–gel refractory coatings on chemically-bonded sand cores for foundry applications to improve casting surface quality. Surf. Coat. Technol. **205**(16), 4035–4044 (2011). https://doi.org/10.1016/j.surfcoat.2011.02.042
13. Ł Jamrozowicz, A. Siatko, The assessment of the permeability of selected protective coatings used for sand moulds and cores. Arch. Foundry Eng. (2019). https://doi.org/10.24425/afe.2020.131276
14. B. Liu, L. Song, W. Liu, X. Yan, The effect of aggregates, binders, and additives on the properties of water-based coatings for foundry and the coating mechanism. Int. J. Met. **19**(1), 176–186 (2025). https://doi.org/10.1007/s40962-024-01268-x
15. N. Kaźnica, J. Zych, Effectiveness of protective action of coatings from moisture sorption into surface layer of sand moulds. Arch. Metall. Mater. **61**(4), 2111–2116 (2016). https://doi.org/10.1515/amm-2016-0283
16. S. Cacace, D. Chiesa, M. Chiesa, P. Parenti, Q. Semeraro, A novel assessment of the thermo-mechanical behavior of chemically bonded 3D-printed sand cores. Int. J. Met. (2025). https://doi.org/10.1007/s40962-025-01652-1
17. R.A. Johnson, D.W. Wichern, *Applied Multivariate Statistical Analysis* (Prentice hall Upper Saddle River, New York, 2002)